WORKING REPORT

By Shengpu Wang

Internship Project in Prof. Alexey Ustinov's Group, KIT

October, 2021

Content

Readout Pulse Shape Optimization by Genetic Algorithm

Summer Internship Project under Dr. Andre Schneider's Supervision

Karlsruhe Institute of Technology, Prof. Alexey Ustinov's Group

Working Report by Shengpu Wang
October, 2021

Abstract

Transmon qubit is a competitive solution to store information in massive quantum circuits. One method of qubit state readout is IQ measurement, or dispersive readout. When the qubit is detuned from the resonator frequency, the qubit induces a state-dependent frequency shift of the resonator from which the qubit state can be inferred by interrogating the resonator. In order to obtain reliable state readout results, the signal-to-noise-ratio should be sufficiently large to suppress separation error. In this experiment, I will introduce a method that maximizes the relative separation between two qubit states through readout pulse shape optimization using genetic algorithm.

1. Brief Description of Experiment Circuit

1.1. Qubit Configuration [1]

By replacing the Conductor in a LC oscillator circuit, the Hamiltonian of the system becomes

$$H = 4E_C\left(n - n_g\right)^2 - E_J \cos\left(2\pi \frac{\phi}{\phi_0}\right)$$

where n is the number operator of Cooper pairs $n = -\frac{q}{2e}$ and $E_C = \frac{e^2}{2C}$. The second term represents the energy stored in Josephson Junction $E_{Jos} = -E_J \cos\left(2\pi \frac{\phi}{\phi_0}\right)$, where ϕ_0 represents the flux quantum $\phi_0 = \frac{h}{2e}$. And n_g is the bias pairs number controlled by DC gate amplitude. This Hamiltonian leads to an energy distribution shown in Figure 1.

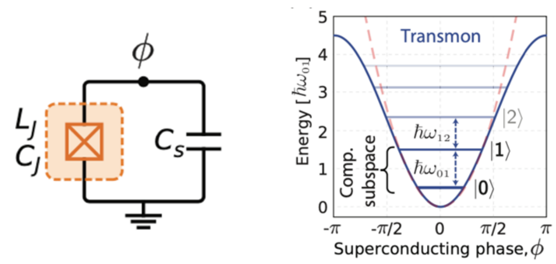

Figure 1. Transmon Qubit Configuration and Energy Level Distribution.

When the driving frequency is close to the difference between first two energy levels, we can approximate the system to a two-level system and if it is coupled to a resonator, the effective Hamiltonian of the system becomes:

$$H_{eff} = \frac{1}{2}\left(\omega_{01} + \frac{g^2}{\Delta}\right)\sigma_z + \left(\omega_r + \frac{g^2}{\Delta}\sigma_z\right)a^\dagger a + \cdots$$

which implies that we can equal this system to a microwave resonator whose resonant frequency depends on qubit state. Derivation of this effective Hamiltonian is shown in Appendix. The frequency response of this analogous resonator is shown below. So, if we send a microwave pulse with a specific frequency into qubit sample and measure the transmission coefficients, we can extract qubit state from the value of transmission coefficients. In most cases, complex transmission coefficients are measured and plotted onto complex plane. Different regions of data points represent the ground and excited qubit state. This method is introduced in the following part.

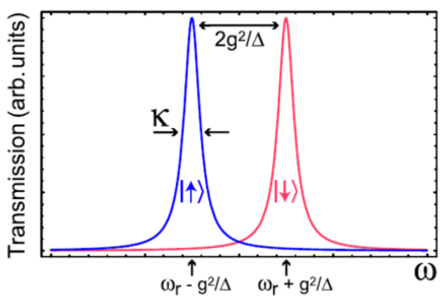

Figure 2. Transmission spectrum of a resonator whose resonant frequency depends on qubit state.[2]

1.2. Measurement Method and Readout Pulse

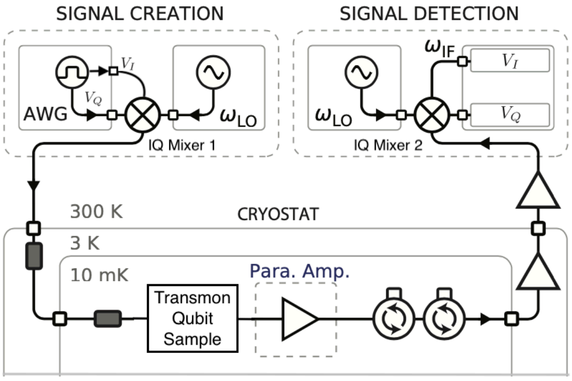

Figure 3. Experiment Circuit Used in Following Parts.[3]

Figure 3 only shows readout part of experiment circuits. Manipulation part is omitted for simplicity. First, AWG generates two quadrature signals with arbitrary unit amplitude:

$$IF = \begin{cases} \cos(\omega_{IF} t) \\ \sin(\omega_{IF} t) \end{cases}$$

and input them to IQ mixer together with signal from a local oscillator, $LO = \sin(\omega_{LO} t)$. So, the signal at qubit sample's input portal is

$$\sin(\omega_{LO} t) \xrightarrow[\sin(\omega_{IF} t)]{\cos(\omega_{IF} t)} \cos(\omega_{LO} t) \cos(\omega_{IF} t) + \sin(\omega_{LO} t) \sin(\omega_{IF} t)$$
$$= \cos\big((\omega_{LO} + \omega_{IF}) t\big).$$

This signal goes through the resonator coupled to the qubit and its amplitude and phase is changed. Theoretically, we have:

$$\cos\big((\omega_{LO} + \omega_{IF}) t\big) \xrightarrow{sample} A \cos\big((\omega_{LO} + \omega_{IF}) t + \phi\big)$$
$$\xrightarrow{\text{IQ mixer}} \begin{cases} \text{multiply with } \cos(\omega_{\mathrm{LO}} t) \text{ and filter out high frequency component} \rightarrow \dfrac{A}{2} \cos(\omega_{IF} t + \phi) \rightarrow \mathrm{V_Q} \text{ output} \\ \text{multiply with } \sin(\omega_{\mathrm{LO}} t) \text{ and filter out high frequency component} \rightarrow \dfrac{\mathrm{A}}{2} \sin(\omega_{IF} t + \phi) \rightarrow \mathrm{V_I} \text{ output} \end{cases}$$

where A and ϕ depend on qubit state. Then V_I and V_Q are decomposed to separated frequency components:

$$V_Q = \left(\frac{A}{4} \cos\phi + \frac{iA}{4} \sin\phi\right) e^{i\omega_{IF} t} + \left(\frac{A}{4} \cos\phi - \frac{iA}{4} \sin\phi\right) e^{-i\omega_{IF} t}$$

$$V_I = \left(-\frac{A}{4} \sin\phi + \frac{iA}{4} \cos\phi\right) e^{i\omega_{IF} t} - \left(\frac{A}{4} \sin\phi + \frac{iA}{4} \cos\phi\right) e^{-i\omega_{IF} t}$$

To analyze experiment data, we calculate Fourier transform result of $V_I(t) + i \cdot V_Q(t)$:

$$\frac{1}{2\pi} \int [V_I(t) + i V_Q(t)] e^{-i\omega_{IF} t} dt$$
$$\propto -\frac{A}{4} \sin\phi + \frac{iA}{4} \cos\phi + i\left(\frac{A}{4} \cos\phi + \frac{iA}{4} \sin\phi\right)$$
$$= \frac{A}{2}(-\sin\phi + i\cos\phi)$$

Then we can plot this result onto a complex plane. Since A and ϕ depend on qubit state, there should be two different clusters of points on complex plane and each of them corresponds to a certain qubit state. According to this procedure, one single shot measurement generates one data point on complex plane. So, if single shot measurement of the same qubit state is repeated for many times, data points number in each cluster shows population in each energy level. For example, if the qubit is prepared in pure $|0\rangle$ or $|1\rangle$ state, all the data points should converge in one cluster. Measurement results of pure state are shown in Figure 4.

1.3. Pulse Shape Optimization

The readout microwave signals sent into qubit sample certainly have finite length in time domain. Usually, readout pulse is generated by multiply a sine function with a rectangular pulse:

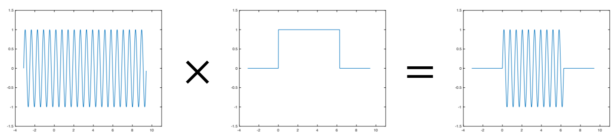

But no evidence proves that rectangular shape is the best pulse shape to do this IQ measurement. For example, a smooth shape can also be used to generate the microwave pulse:

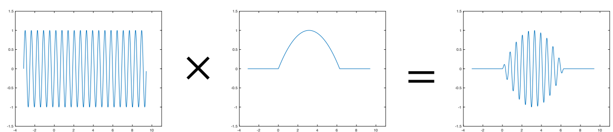

In following parts, the goodness of IQ measurement is quantified by SNR (or Readout Fidelity) and Genetic Algorithm is used to search for pulse shapes that can increase measurement SNR. The results show that there do exist pulse shapes better than rectangular shape.

2. Genetic Algorithm

2.1. Definition of SNR and Readout Fidelity

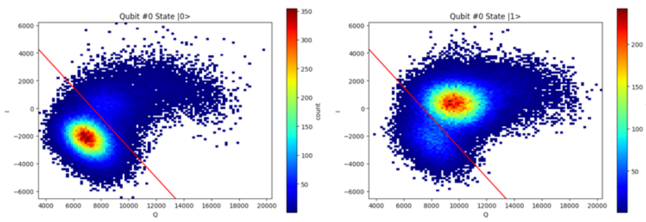

Figure 4. IQ measurement result, also known as IQ clouds. First, the qubit is prepared in $|0\rangle$ state and we measure it using IQ signal method. The result is shown in left figure and we can see most of the points converge in a specific region represents state $|0\rangle$. Then we apply a Pi-Pulse to the qubit, which swaps the population of state $|0\rangle$ and state $|1\rangle$, and measure again. The points in right figure converge in another region represents state $|1\rangle$.

Because of thermal and electromagnetic noise in cryostat, points represent IQ measurement results are distributed in a specific region following Gaussian Distribution. Figure 1 shows a practical result from experiment. To analyze the results and distinguish qubit state, we fit the distribution in Figure 1 using Gaussian Distribution Model so we can extract the mean value and standard deviation of each distribution. Then we define:

$$SNR = \frac{|\mu_{|0\rangle} - \mu_{|1\rangle}|}{\sigma_{|0\rangle} + \sigma_{|1\rangle}}$$

and

$$Readout\ Fidelity = \mathrm{erf}\left(\frac{SNR}{\sqrt{2}}\right)$$

to quantify the goodness of a measurement, where $\mu_{|0\rangle}$, $\mu_{|1\rangle}$ are the mean value of $|0\rangle$, $|1\rangle$ cloud, shown in Figure 4, and $\sigma_{|0\rangle}$, $\sigma_{|1\rangle}$ are the standard deviation of each cloud. The reason why we choose those parameters is obvious: the farther the distance between clusters correspond to different qubit states and the smaller the standard deviation of each distribution, the easier can we distinguish the qubit state by data point's position from a single shot measurement.

2.2. Flow Chart of GA

Just as the name of this algorithm indicates, it imitates the evolution of real species in nature. In a real ecosystem, only the creatures who fit the environment well survive and pass on their DNA to the next generation. During this process the individuals in one cluster become stronger and stronger and as a result, the nature selects those individuals who have better performance to survive. In genetic algorithm, individuals are pulses with different shapes and every pulse has its own DNA which will be discussed later. To select shapes which lead to better experiment results, the algorithm chooses those pulses with better performance and creates another generation according to their DNA. Later we will see that a 50-generation evolution can give out a decent progress.

In my experiment, the cluster of this "pulse species" has twenty individuals in one generation and each of them has their own DNA. Then the algorithm does IQ measurement using those pulses and records SNR for every pulse shape, which represent their fitness to environment. The pulses with higher SNR are more probable to be selected as parents to breed next generation: if two pulses are selected as parents, the algorithm exchange their DNA to create two new pulses during which mutations may happen with a certain probability. That is basically how the evolution goes on. Details will be discussed later.

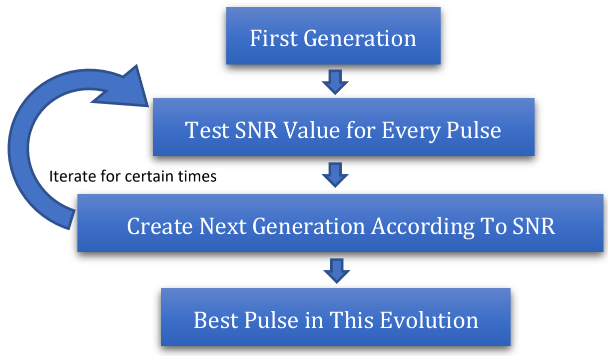

Figure 5. Flow Chart of Genetic Algorithm.

2.2.1. Encode Pulse Shape

In order to realize the evolution, we need a way to determine a pulse shape by a sequence of numbers. Binary encoding method fits Genetic Algorithm well, especially in mutation process, so I decide to encode pulse shapes by binary digits. To encode a pulse shape, pulse length is divided into several time zone, and in each time zone the amplitude remains the same. Then the relative amplitude of every time zone is determined by a binary number. In this way, by piece together all those binary numbers, the shape of pulse is completely determined. The more the number of time zones and the more digits of binary numbers describing amplitude in each time zone, the more precise can we determine the pulse shape. The left picture shown below is a simplified example of this encoding protocol.

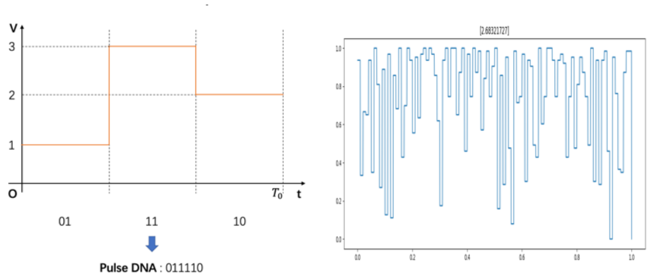

Figure 6. Encoding method example and real encoded pulse in Genetic Algorithm.

In Figure 6's left picture, the pulse shape is depicted by a six-digit binary code:

a) Encoding Method: Pulse length is divided into three time zones, and the amplitude of each time zone is determined by a two-digit binary number. In this case, 11 represents the maximum voltage of current experiment setting.

b) For 011110, 01 represents the amplitude in the first time zone and 11, 10 represent the amplitudes in following time zones.

c) Depict the amplitude in each time zone and we get the shape in Figure 6.

Until now we only determine the relative amplitude of a pulse shape. The actual amplitude and pulse length are determined by power attenuation parameter in Frontend Box and single qubit characterization separately. In this experiment, the attenuation is several dB and the actual pulse length is 416 ns. Since there are only six digits that we use to determine a pulse shape in this example, only simplest shapes can be described by this encoding method. To improve precision and resolution during experiment, the pulse length is divided into 100 time zones and amplitude in each time zone is determined by a six-digit binary number. So, in total six hundred digits are used to describe a pulse shape, which is the "DNA" of a pulse shape. A pulse shape example determined by this protocol from experiment is depicted in the right picture in Figure 6.

2.2.2. First Generation Initialization

Before this evolution start, we need to create the first generation manually. In this experiment, the first generation consists of pulses with usual shapes (Gaussian, rectangular, step, exponential decay, shown in Figure 7).

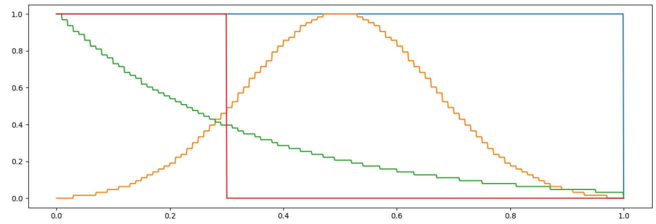

Figure 7. The First Generation of Evolution. There are five individuals of every pulse shape in this figure, so, in total there are 20 individuals in one generation. Every individual is determined by a 600-digit DNA.

2.2.3. Reproduction and mutation [4]

With the first generation, this algorithm does IQ measurement with every pulse shape in the first generation and records SNR values of them. Then the algorithm chooses parents for next generation: the probability of a pulse shape to be chosen is proportional to its SNR value. So, the higher the SNR value of a pulse shape, the more probable it is to be chosen by the algorithm. The algorithm chooses two pulses at one time and once two pulses are chosen, they are used to breed two new individuals. There are two probabilities:

a) By 30%, their offspring are the same with the parents.

b) By 70%, These two individuals exchange part of their DNA at a random position.

After two new DNAs are generated either by one of these two ways, every digit in new DNAs may switch to the opposite (from 0 to 1 or from 1 to 0) with probability 0.5%. This process is shown in Figure 8.

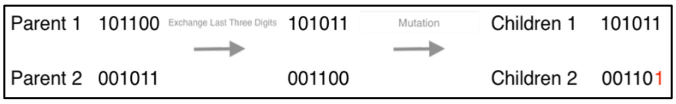

Figure 8. Reproduction Procedure, from one generation to the next one.

This procedure is repeated by 10 times and each time two new individuals are generated. So, we have 20 new individuals and they are the second generation in this evolution. Their SNR values are tested and they go through the same reproduction procedure again to generate the third generation.

During this evolution, from generation to generation, the measurement goodness using pulse shapes in every generation are recorded and they are shown in the next part.

3. Results from Genetic Algorithm

3.1. Experiment Results

Here is a typical comparison between rectangular pulse and best pulse found by Genetic Algorithm (GA pulse).

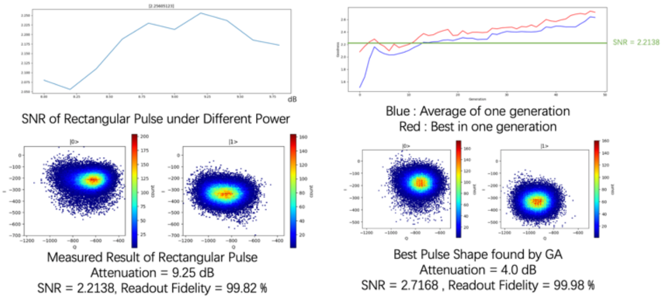

Figure 9. Comparison between rectangular pulse and GA pulse.

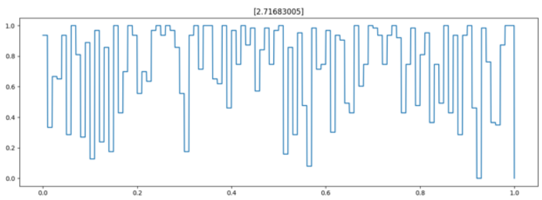

Figure 10. The best pulse shape found by Genetic Algorithm, corresponding to results in Figure 9.

In left, the upper picture shows SNR value of rectangular pulse under different power attenuation settings and the lower one shows IQ clouds result under the optimal attenuation setting. The best measurement SNR value is 2.2138 under Attenuation = 9.25 dB. To find better pulse shapes using Genetic Algorithm, the power attenuation should be lower to increase maximum voltage of real microwave signal in experiment circuit. In this execution, the power attenuation was 4.00 dB and the evolution lasts for 50 generations. In right part of Figure 9, the result of evolution is shown. Clearly, measurement goodness increases with generation and surpasses the best performance of rectangular pulse marked by the green line. The best pulse shape found by GA achieves SNR value equals to 2.7168 and Readout Fidelity is increased by 0.16%. From the IQ clouds shown in Figure 9, we can see that the points distribution in right picture is more condensed and later I will show that the distance between two clouds is farther, too.

Here are more results from experiment. Since the qubit status is always shifting (For example, in last result the best performance of rectangular pulse is 2.2138 but three days after the best performance dropped to about 1.4 and the resonant frequency of coupled resonator shifted from 8.575547 GHz to 8.577054 GHz.), I want to make sure that this algorithm works under all circumstances through more tests.

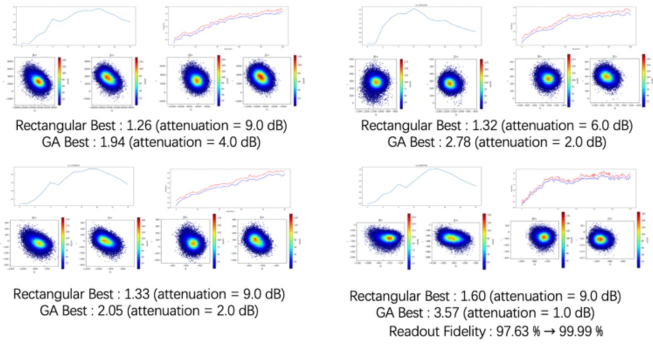

Figure 11. More results from experiment. Genetic Algorithm gives out better performance under every condition.

Among all this results, the last one is the most representative: 1.60 is a typical SNR value of rectangular pulses in most cases and this evolution lasts for 300 generations while others only last for 50 or 100 generations. We can see that in the last stage of evolution, SNR values converge to a specific value which is much higher than that of rectangular pulse. This result can be a persuasive evidence proves that Genetic Algorithm is very helpful in searching for better readout pulse shapes.

3.2. Why GA Pulse is better?

In previous section, we only see that the SNR value of measurement is improved and, in this section, I will show how this happens. First of all, the SNR is defined by

$$SNR = \frac{|\mu_{|0\rangle} - \mu_{|1\rangle}|}{\sigma_{|0\rangle} + \sigma_{|1\rangle}},$$

as we discussed before. To investigate why SNR increases with generations, I recorded the mean values and standard deviations of Gaussian distributions during evolution. The results are shown in Figure 12.

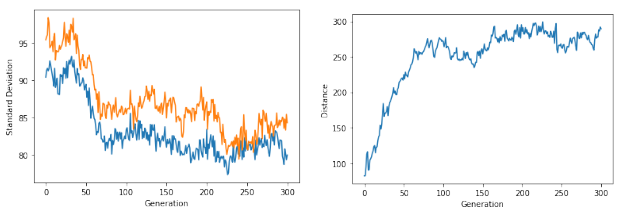

Figure 12. Standard Deviation (left) and Distance between $|0\rangle$ Cloud and $|1\rangle$ Cloud (right).

Just as we expected, the distance between two clouds ($|\mu_{|0\rangle} - \mu_{|1\rangle}|$) increases while the standard deviations ($\sigma_{|0\rangle}$ and $\sigma_{|1\rangle}$) of two distributions decrease. As a result, total SNR increases with evolution goes on.

3.3. Further Investigation.

3.3.1. Rabi Measurement with GA pulses.

Since GA pulses have those advantages over rectangular pulse, I used it to do a Rabi measurement. In this measurement, instead of preparing qubits in pure $|0\rangle$ or $|1\rangle$ state using a Pi Pulse, I applied manipulation pulses with different length and theoretically, the qubit should swing between two states. So, if the qubit stays in a superposition state, sine the two clouds measured in previous section are well separated, the IQ clouds measurement should give out two clusters on complex plane, representing population in ground and excited state separately. Unfortunately, until now I can't see such distribution pattern. Here is the measurement result after applying a Pi-Half Pulse. Theoretically, qubit population are evenly distributed in ground and excited state, so, half of data points should be in one region representing ground state on complex plane while half of data points should be in another region. But according to the experiment result, the only difference is that all data points are distributed in a larger region, so in this aspect, best pulses found by Genetic Algorithm don't outperform rectangular pulse.

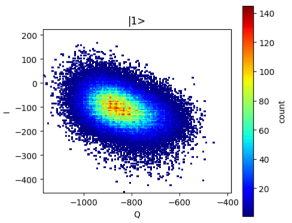

Figure 13. Measurement result after Pi-Half Pulse. Data points are distributed in a larger region, instead of two separated clusters.

Another explanation for this phenomenon may be kind of embarrassing: actually, I'm not very skilled at using *Qicode*, the hardware controlling language we use in our lab; Since the measurement of pure state is quite convincing, there is also chances that I was not using *Qicode* correctly during Rabi measurement.

3.3.2. Fourier Spectrum of GA Pulse.

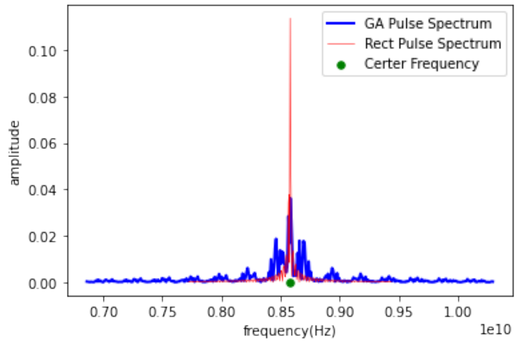

Figure 14. Fourier Spectrum of rectangular pulse and GA pulse. Center Frequency = 8577054373.086808 *Hz.*

Because the microwave pulse we send into the sample is only a part of sine function (shaped by rectangular pulse or pulse found by GA), the spectrum of shaped pulse has other frequencies' components other than center frequency. Figure 14 shows Fourier analysis results of rectangular pulse and GA pulse. This result is surprising because rectangular pulse's spectrum is more condensed and GA pulse's spectrum has obvious parasitic frequency components. Since theoretically, we should only use mono-frequency pulse to probe the qubit state, a more distributed spectrum is really out of expectation.

4. Reference

[1] P. Krantz, M. Kjaergaard, F. Yan, T. P. Orlando, S. Gustavsson, and W. D. Oliver, "A quantum engineer's guide to superconducting qubits", Applied Physics Reviews 6, 021318(2019) https://doi.org/10.1063/1.5089550

[2] T. Wirth, J. Lisenfeld, A. Lukashenko, A. V. Ustinov, "Dispersive readout scheme for a Josephson phase qubit", arXiv:1010.0954v1

[3] Sorin Paraoanu, Aydar Sultanov, "Readout techniques for superconducting qubits", Lecture Notes.

[4] Melanie Mitchell, "An Introduction to Genetic Algorithms", MIT Press, First Edition (1998), https://mitpress.mit.edu/books/introduction-genetic-algorithms

Learning Notes

1. About Readout Circuits

1.1. Physical Background of Dispersive Readout

First of all, we use Josephson Junction to replace the inductance in a LC oscillator and as a result we can create anharmonicity in the energy level of the system. In a LC oscillator, the Hamiltonian of the system is

$$H = \hbar\omega\left(a^{\dagger}a + \frac{1}{2}\right)$$

which leads to an even distributed eigen energy levels. To create (approximately) two-level systems, Josephson Junction replaces the inductance and the Hamiltonian becomes

$$H = 4E_C\left(n - n_g\right)^2 - E_J\cos\left(2\pi\frac{\phi}{\phi_0}\right)$$

where n is the number operator of Cooper pairs $n = -\frac{q}{2e}$ and $E_C = \frac{e^2}{2C}$. The second term represents the energy stored in Josephson Junction $E_{Jos} = -E_J\cos\left(2\pi\frac{\phi}{\phi_0}\right)$, where ϕ_0 represents the flux quantum $\phi_0 = \frac{h}{2e}$. And n_g is the bias pairs number controlled by DC gate voltage.

The ration $\frac{E_J}{E_C}$ determines the type of qubits. If it is small the qubit is called cooper-pair box and if it is large the qubit is transmon qubit which is the qubit we use in our lab.

Denote operators n and ϕ by the following form

$$n = \frac{i}{2}\sqrt{\hbar}\sqrt[4]{\frac{E_J}{2E_C}}\left(b - b^{\dagger}\right)$$

$$\phi = \sqrt{\hbar}\sqrt[4]{\frac{2E_C}{E_J}}\left(b + b^{\dagger}\right)$$

The Hamiltonian becomes

$$H = \sqrt{8E_CE_J}\left(bb^{\dagger} + \frac{1}{2}\right) - E_J - \frac{1}{12}E_C\left(b^{\dagger} + b\right)^4$$

which leads to unevenly distributed energy levels. See figure.1.[1]

[1] A Quantum Engineer's Guide to Superconducting Qubits

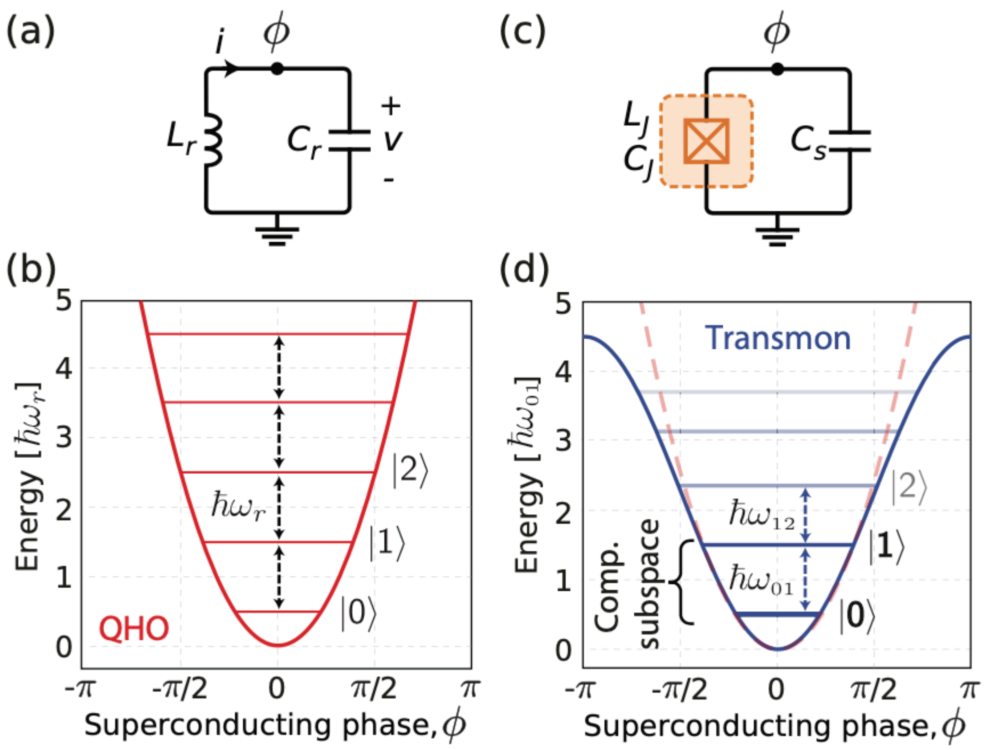

Figure 1. Transmon Qubit's Configuration

If the driven frequency is close to the first energy difference, we can approximate the Hamiltonian to a two-level system

$$H = \frac{\omega_{01}\sigma_z}{2}$$

According to Jaynes-Cummings Model, the total Hamiltonian of the qubit and the coupled resonator is

$$H_{total} = \frac{\omega_{01}\sigma_z}{2} + \omega_r a^\dagger a + g(\sigma_+ a + \sigma_- a^\dagger)$$

The eigenstates and eigenenergy of this Hamiltonian can be found in this article[2]

Using S-W-Formalism, this Hamiltonian can be transformed as

$$H_{eff} = \frac{1}{2}\left(\omega_{01} + \frac{g^2}{\Delta}\right)\sigma_z + \left(\omega_r + \frac{g^2}{\Delta}\sigma_z\right)a^\dagger a + \cdots$$

Then the effective resonant frequency of the resonator is dependent on the state of the qubit. By measuring the reaction of the resonator to a specific frequency, we can acquire the state of the qubit. See figure.2.[3]

2 Improving transmon qubit readout using squeezed radiation.
3 Improving transmon qubit readout using squeezed radiation.

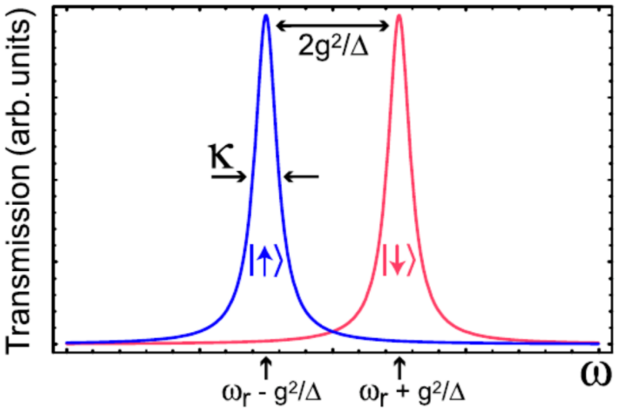

Figure.2. State Dependent Transmission Spectrum of the Resonator

1.2. Dispersive Readout

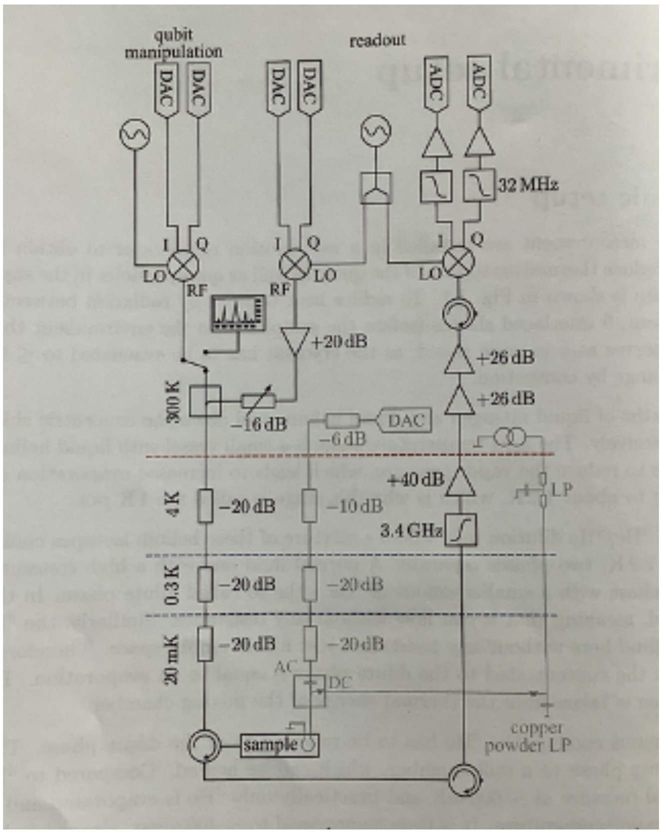

Figure.3. Dispersive Readout Set Up[4]

There are two kinds of signal go into the sample. The manipulation signal is generated by the left IQ mixer in the picture and this signal aimed to control the state of the qubits. While the readout signal is generated by the IQ mixer in the middle. First, the local oscillator generates the LO signal

$$LO = \sin(\omega_{LO} t)$$

And the DACs above it generate quadrature signals

4 Dr. Andre Schneider Master thesis

$$IF = \begin{cases} \cos(\omega_{IF}t) \\ \sin(\omega_{IF}t) \end{cases}$$

The signal sent into the sample is the result of IQ mixer

$$\sin(\omega_{LO}t) \xrightarrow[\sin(\omega_{IF}t)]{\cos(\omega_{IF}t)} \cos(\omega_{LO}t)cos(\omega_{IF}t) + \sin(\omega_{LO}t)\sin(\omega_{IF}t) = \cos\big((\omega_{LO} + \omega_{IF})t\big)$$

This signal goes through the resonator coupled to the qubit and will be changed by the transmission coefficient of the resonator, theoretically:

$$\cos\big((\omega_{LO} + \omega_{IF})t\big) \xrightarrow{sample} A\cos\big((\omega_{LO} + \omega_{IF})t + \phi\big)$$

$$\xrightarrow{\text{IQ mixer}} \begin{cases} \text{multiply with } \cos(\omega_{\mathrm{LO}}\mathrm{t}) \text{ and filter out high frequency component} \rightarrow \dfrac{A}{2}\cos(\omega_{IF}t + \phi) \rightarrow \text{Q output} \\ \text{multiply with } \sin(\omega_{\mathrm{LO}}\mathrm{t}) \text{ and filter out high frequency component} \rightarrow \dfrac{\mathrm{A}}{2}\sin(\omega_{IF}t + \phi) \rightarrow \text{I output} \end{cases}$$

In most cases, the output signal has a continuum spectrum.
The I, Q output can be decomposed by Fourier transformation

$$Q = \left(\frac{A}{4}\cos\phi + \frac{iA}{4}\sin\phi\right)e^{i\omega_{IF}t} + \left(\frac{A}{4}\cos\phi - \frac{iA}{4}\sin\phi\right)e^{-i\omega_{IF}t}$$

$$I = \left(-\frac{A}{4}\sin\phi + \frac{iA}{4}\cos\phi\right)e^{i\omega_{IF}t} - \left(\frac{A}{4}\sin\phi + \frac{iA}{4}\cos\phi\right)e^{-i\omega_{IF}t}$$

Under Fourier transformation on $I(t) + iQ(t)$, we get the results:

$$\int [I(t) + iQ(t)]e^{-2\pi ift}dt \sim -\frac{A}{4}\sin\phi + \frac{iA}{4}\cos\phi + i\left(\frac{A}{4}\cos\phi + \frac{iA}{4}\sin\phi\right) = \frac{A}{2}(-\sin\phi + i\cos\phi)$$

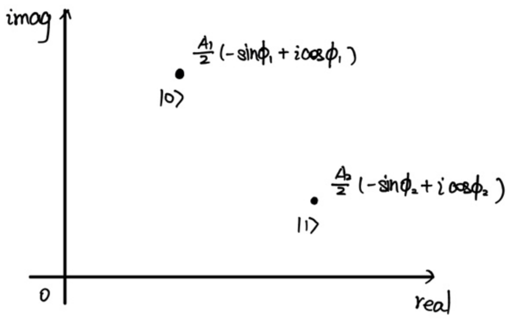

Figure. Different qubit states cause different amplification and phase shift. If plot the real and imaginary part of Fourier analysis results on the complex plane, cluster of points can indicate the qubit state.

If we plot this result on a complex plane, the amplification and phase shift related to the state of the qubit, A and ϕ, will determine the location of the data points. Then $|0\rangle$ and $|1\rangle$ will create two clusters on the plane. Using clustering algorithms, we can distinguish the state of the qubit by the clusters on the signal plane.

1.3. Details about analog-digital readout

Shannon sampling theorem

When converting an analog signal $x(t)$ to digital signal, a sample pulse train $p(t)$ is needed and the readout result is

$$x_s(t) = x(t)p(t)$$

where

$$p(t) = \sum_{n=-\infty}^{\infty} \delta(t - nT).$$

And T corresponds to sample rate

$$\omega_0 = \frac{2\pi}{T} = 2\pi f_s$$

Fourier Analysis of $p(t)$ is

$$p(t) = \sum_{k=-\infty}^{\infty} \frac{1}{T} e^{jk\omega_0 t}$$

leads to

$$x_s(t) = \sum_{k=-\infty}^{\infty} \frac{1}{T} x(t) e^{jk\omega_0 t}$$

The Fourier transformation of analog signal $x(t)$ and digitalized signal $x_s(t)$ is

$$X(f) = \sum_{k=-\infty}^{\infty} \frac{1}{T} \int_{-\infty}^{\infty} x(t) e^{-j2\pi f t} dt$$

$$X_s(f) = \sum_{k=-\infty}^{\infty} \frac{1}{T} \int_{-\infty}^{\infty} x(t) e^{-j2\pi f t} dt$$

Then

$$X_s(f) = \frac{1}{T} \sum_{k=-\infty}^{\infty} X(f - kf_s) = \cdots + \frac{1}{T} X(f + f_s) + \frac{1}{T} X(f) + \frac{1}{T} X(f - f_s) \cdots$$

If there is a low-pass filter to limit the frequency band width of original signal, the sampling frequency must satisfy

$$f_s \geq 2 f_{max}$$

Or terms $\frac{1}{T} X(f + f_s)$, $\frac{1}{T} X(f)$, $\frac{1}{T} X(f - f_s)$ will overlap with each other and it is impossible to obtain the original frequency spectrum of analog signal.

Reference: *Digital Signal Processing (Third Edition), 2019, Lizhe Tan, Jean Jiang*

Digital Down conversion

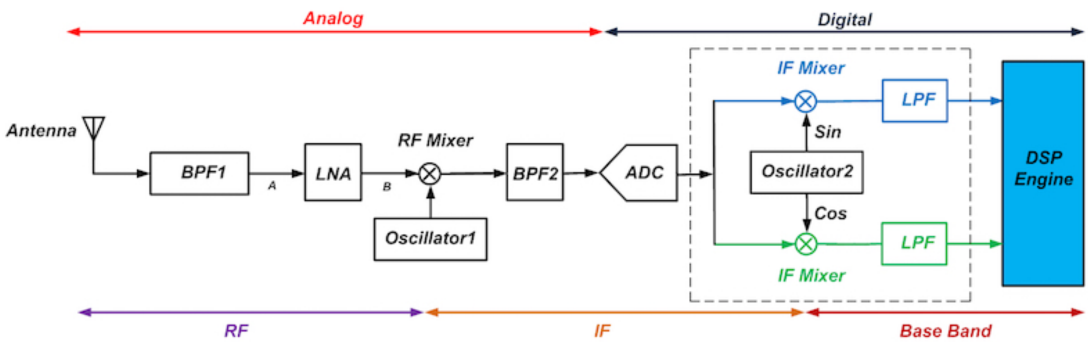

Figure.4. Diagram of Digital Down Conversion (DDC)

The desired analog signal comes from Antenna and the BPF1(Bandpass filter) and RF mixer convert it to frequency f_{IF}. Then the analog signal is converted to digital domain by ADC. The Oscillator2 will generate digital signal corresponds to sin and cos, with a frequency $f = f_{IF}$. If the digitized signal after ADC has a spectrum shown in Figure.5.

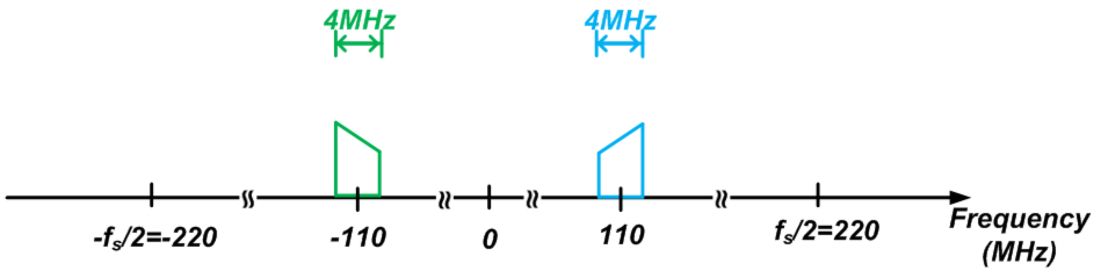

Figure.5. Spectrum of Digitized Signal

After multiplication with signal from Osillator2, the spectrum becomes

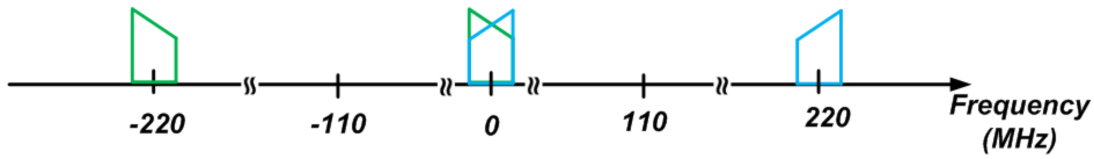

Figure.6. Spectrum of the Signal after IF mixer

We can use Figure.6. to describe the spectrum of signals both in upper and lower lines in Figure.4. because they have the same amplitude distribution, but there is a quadrature phase shift between the two signals. Then the LPFs only pass signals between $-2MHz$ and $2MHz$. Although the amplitude distribution overlaps around DC, the phase difference caused by sin and cos can help us distinguish the amplitude distribution and reconstruct the original signal.

Reference: Website *All About Circuits*, https://www.allaboutcircuits.com/technical-articles/dsp-basics-of-digital-down-conversion-digital-signal-processing

But the process we use in the readout is different from DDC. As shown in Figure.3, we plot the IQ signal on a complex plane, with I signal as real coordinate and Q signal as imaginary coordinate. Theoretically, the sampling points will rotate at an angular velocity $\omega = \omega_{IF}$. So, if we multiply $e^{-i\omega_{IF}t}$ to each point, the rotating can be offset and the points should converge at a specific point determined by the amplification and phase shift by qubit sample. Then we can distinguish the state by the converge points of the offset IQ cloud. This algorithm is carried out by *IQ_cloud_analysis.py* in qkit package. This process can be shown in the following figure.

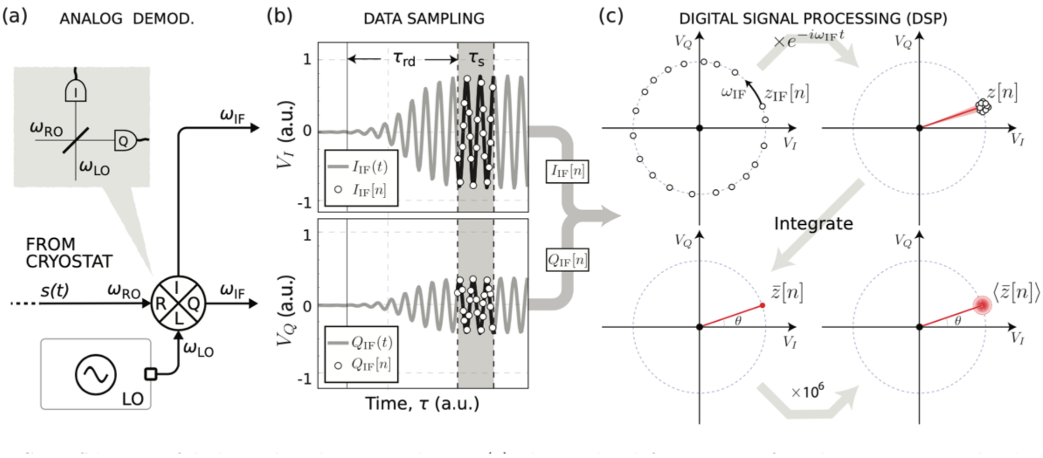

Figure.7. Down Conversion of I-Q Signal[5]

2. Clustering Algorithms

In both ways of processing IQ signals, Fourier Transformation and Down Conversion, the state of qubits is represented by clusters of data points in complex plane. And the way to distinguish two clusters is not always easy. Here I investigate several useful clustering algorithms and I'm going to test them in the following experiment.

2.1. Gaussian mixture model with Expectation Maximization (EM) clustering

First of all, Gaussian probability distribution function is

$$N(x;u,\Sigma)=\frac{1}{\sqrt{2\pi|\Sigma|}}\exp\left[-\frac{1}{2}(x-u)^T\Sigma^{-1}(x-u)\right]$$

where x is the n-dimension vector represents sample point's coordinate and u is the vector represents the center of the distribution with the same dimension. Σ is the covariance matrix and different type of Σ describes different distributions (specifically, spherical covariance matrix is diagonal and represents a spherical distribution).

Gaussian Mixture model views the data as summation of K different $N(x;u,\Sigma)$, which means

$$\Pr(x)=\sum_{k=1}^{K}\pi_k N(x;\mu_k,\Sigma_k)$$

π_k is the weight of each distribution whose summation equals one. The process to find the optimal parameters μ_k,Σ_k is maximize the Likelihood Function

$$LF=\prod_{i=1}^{N}\Pr(x_i;\theta)$$

Usually, we deal with

$$\sum_{i=1}^{N}\log\Pr(x_i;\theta)$$

Now we use an iteration to optimize parameters.

First, we define

$$\gamma(i,k)=\frac{\pi_k N(x_i;u_k,\Sigma_k)}{\sum_{j=1}^{K}\pi_j N(x_i;u_j,\Sigma_j)}$$

5 A Quantum Engineer's Guide to Superconducting Qubits

This is the probability that point i is generated by cluster k. Then the number of points belong to this cluster is

$$N_k = \sum_{i=1}^{N} \gamma(i,k)$$

The center (or the center of weight) of cluster k is

$$u_k = \frac{1}{N_k} \sum_{i=1}^{N} \gamma(i,k) x_i$$

The covariance matrix

$$\Sigma_k = \frac{1}{N_k} \sum_{i=1}^{N} \gamma(i,k)(x_i - u_k)(x_i - u_k)^T$$

Then we revise the weight of each cluster by

$$\pi_k = \frac{N_k}{N}$$

and continue this process until the results of different steps converge.

2.2. Fuzzy c-means clustering algorithm

This algorithm works with highly overlapped points distribution and attributes each point an array, which describes the probability of this point belongs to each cluster. Consequently, the summation of these probabilities should be one.

Let $X = \{x_1, x_2, \cdots, x_n\}$ be the set of data points and $V = \{v_1, v_2, \cdots, v_c\}$ be the set of centers. At beginning we randomly selected c centers. With these centers we can calculate the fuzzy membership μ_{ij} using

$$\mu_{ij} = 1 / \sum_{k=1}^{c} \left(\frac{d_{ij}}{d_{ik}} \right)^{\frac{1}{m-1}}$$

where d_{ij} is the Euclidean distance between i^{th} data and j^{th} cluster center. m is the fuzziness index ($m \geq 1$). c is the number of cluster centers.

Then the cluster centers will be adjusted through

$$v_j = \frac{\sum_{i=1}^{n} \mu_{ij}^m x_i}{\sum_{i=1}^{n} \mu_{ij}^m}, \qquad \forall j = 1,2,\cdots,c$$

This process goes on until the results converge.

3. Learning notes about J-C Model

3.1. Different pictures of motion

In Schrödinger picture, the state vector change with time while the operator remains the same. The time evolution of vectors is described by a unitary operator $U(t, t_0)$ and

$$|\psi(t)\rangle = U(t, t_0)|\psi(t_0)\rangle$$

Because of Schrödinger equation

$$i\hbar \frac{\partial}{\partial t} |\psi(t)\rangle = H|\psi(t)\rangle$$

then

$$U(t) = e^{-\frac{iHt}{\hbar}}$$

if the Hamiltonian doesn't depend explicitly on time.

When H depends on time and commutes with itself at different time, then

$$U(t) = \exp\left(-\frac{i}{\hbar}\int_0^t H(t')dt'\right)$$

In Heisenberg pictures, the state vector remains the same while the operator changes. The operator changes with time in the following form:

$$A(t) = U^\dagger(t)AU(t)$$

A is the operator in Schrödinger picture. If H doesn't vary with time, then there is

$$\frac{d}{dt}A(t) = \frac{i}{\hbar}[HA(t) - A(t)H] + e^{\frac{iHt}{\hbar}}\frac{\partial A}{\partial t}e^{-\frac{iHt}{\hbar}}$$

This equation can be solved in this form

$$A(t) = A + \frac{it}{\hbar}[H, A] + \frac{1}{2!}\left(\frac{it}{\hbar}\right)^2 [H, [H, A]] + \cdots$$

In the Interaction picture (Dirac picture), both vector and operator carry time dependence. Usually, the Hamiltonian will be split into two parts

$$H_S = H_{0,S} + H_{1,S}$$

and the first term has no time dependence. Then the state vector and operator evolution is defined as

$$|\psi_I(t)\rangle = e^{\frac{iH_{0,S}t}{\hbar}}|\psi_S(t)\rangle$$

$$A_I(t) = e^{\frac{iH_{0,S}t}{\hbar}}A_S(t)e^{-\frac{iH_{0,S}t}{\hbar}}$$

Specifically, for the Interaction picture Hamiltonian, we have

$$H_{0,I}(t) = H_{0,S}(t)$$

$$H_{1,I}(t) = e^{\frac{iH_{0,S}t}{\hbar}}H_{1,S}(t)e^{-\frac{iH_{0,S}t}{\hbar}}$$

According to Schrödinger Equation, the interaction vector and operator satisfy

$$i\hbar\frac{d}{dt}|\psi_I(t)\rangle = H_{1,I}(t)|\psi_I(t)\rangle$$

And if A_S is time-independent, time evolution of $A_I(t)$ is

$$i\hbar\frac{d}{dt}A_I(t) = [A_I(t), H_{0,S}]$$

3.2. JC model[6]

The Hamiltonian of an interaction system consists of a resonator and a two-level system (usually atom, transmon qubit two-level system in our experiment) is

$$H = H_{field} + H_{atom} + H_{int}$$

where

$$H_{field} = \hbar\omega_c a^\dagger a, H_{atom} = \hbar\omega_a\frac{\sigma_z}{2}, H_{int} = \frac{\hbar\Omega}{2}(a + a^\dagger)(\sigma_+ + \sigma_-)$$

$$\sigma_+ = |e\rangle\langle g|, \sigma_- = |g\rangle\langle e|$$

Using Interaction picture and denoting $H_0 = H_{field} + H_{atom}$, the interaction Hamiltonian is

$$H_{int}(t) = H_{0,I}(t) + H_{1,I}(t) = \frac{\hbar\Omega}{2}\left[a\sigma_- e^{-i(\omega_c+\omega_a)t} + a^\dagger\sigma_+ e^{i(\omega_c+\omega_a)t} + a\sigma_+ e^{-i(-\omega_c+\omega_a)t} + a^\dagger\sigma_- e^{i(-\omega_c+\omega_a)t}\right]$$

Neglecting quickly oscillating terms and transforming back to Schrödinger picture, we have

6 Improving transmon qubit readout using squeezed radiation.

$$H_{JC} = \hbar\omega_c a^\dagger a + \hbar\omega_a \frac{\sigma_z}{2} + \frac{\hbar\Omega}{2}(a\sigma_+ + a^\dagger\sigma_-)$$

Choose

$$H_I = \hbar\omega_c \left(a^\dagger a + \frac{\sigma_z}{2}\right)$$

$$H_{II} = \hbar(\omega_a - \omega_c)\frac{\sigma_z}{2} + \frac{\hbar\Omega}{2}(a^\dagger\sigma_- + a\sigma_+)$$

The eigenstates of H_I, $|\psi_{1n}\rangle = |n, e\rangle$ and $|\psi_{2n}\rangle = |n+1, g\rangle$, construct a subspace and we can re-diagonalize Hamiltonian operator in this subspace:

$$|n, +\rangle = \cos\left(\frac{\alpha_n}{2}\right)|\psi_{1n}\rangle + \sin\left(\frac{\alpha_n}{2}\right)|\psi_{2n}\rangle$$

$$|n, -\rangle = \sin\left(\frac{\alpha_n}{2}\right)|\psi_{1n}\rangle + \cos\left(\frac{\alpha_n}{2}\right)|\psi_{2n}\rangle$$

where

$$\alpha_n = \tan^{-1}\left(\frac{\Omega\sqrt{n+1}}{\delta}\right)$$

When put an atom in a resonator, the state of system will evolve following the eigenstates above.

3.3. S-W-Formalism[7]

A system Hamiltonian can always be divided into two parts: block diagonal part and off-diagonal part. As shown in figure.8.

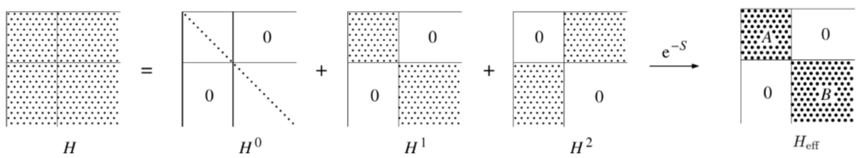

Figure.8. Diagram of S-W-Formalism

For example, if H is divided as described above, we have

$$H = H^0 + \epsilon V$$

ϵ is one order smaller than H^0. The Schrieffer-Wolff transformation

$$H_{eff} = e^{-S}He^{S}$$

aimed at converting H to H_{eff}, which is block off-diagonal to the first order of ϵ. Applying S-W-Formalism on JC model, we divide H_{JC} as

$$H = \underbrace{\omega_r a^\dagger a - \frac{\omega_q}{2}\sigma_z}_{H^0} + \underbrace{g(a^\dagger\sigma_- + a\sigma_+)}_{H'=\epsilon V}$$

We can divide the eigenfunctions of H^0 by the state of the two-level system into two subsets, and in this case H' only interacts states between the two subsets, which means H' is a block off-diagonal matrix. See figure.9.

[7] Perturbative analysis of two-qubit gates on transmon qubits

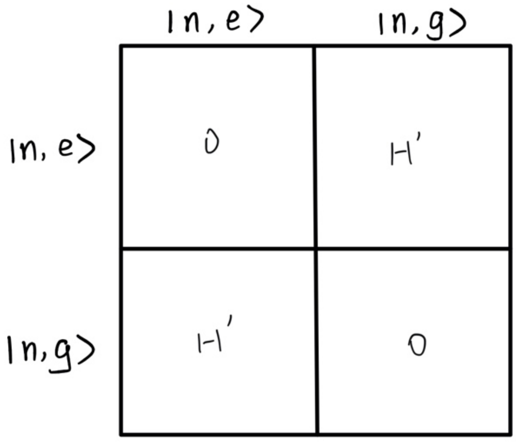

Figure.9. Block Off-Diagonal Matrix H'

We choose the ansatz

$$S^{(1)} = \alpha a^\dagger \sigma_- - \alpha^* a \sigma_+$$

It leads to

$$S^{(1)} = -\frac{g}{\Delta}(a^\dagger \sigma_- - a\sigma_+)$$

The first correction to H^0 is

$$H_{eff} = H^0 + \frac{1}{2}[H^2, S^{(1)}] = \left(\omega_r + \frac{g^2}{\Delta}\sigma_z\right)a^\dagger a - \frac{1}{2}\left(\omega_q - \frac{g^2}{\Delta}\right)\sigma_z$$

Higher order correction of H can be found in Reference 7. In the Hamiltonian above, there is a frequency shift of the resonator caused by $\omega_r + \frac{g^2}{\Delta}\sigma_z$ and an AC stark shift of the qubit energy levels caused by $\omega_q - \frac{g^2}{\Delta}$.

The photon number in the resonator caused by driving microwave is related to the amplitude of driving frequency by

$$n(\omega) = \frac{\kappa}{\left(\frac{\kappa}{2}\right)^2 + (\omega - \omega_{cav})^2} n_{in}(\omega)$$

When driving the resonator with a frequency at resonant and the cavity resonant frequency is shifted by the qubit $\omega_{cav} = \omega_r \pm \chi$, the photon number becomes

$$n(\omega) = \frac{\kappa}{\left(\frac{\kappa}{2}\right)^2 + \chi^2} n_{in}(\omega)$$